

# A 95 GeV Higgs boson and spontaneous CP-violation at the finite temperature

Jing Gao, Xiao-Fang Han, Jinghong Ma, Lei Wang, Haotian Xu

*Department of Physics, Yantai University, Yantai 264005, P. R. China*

## Abstract

The ATLAS and CMS collaborations reported a diphoton excess in the invariant mass distribution around the 95.4 GeV with a local significance of  $3.1\sigma$ . Moreover, there is another  $2.3\sigma$  local excess in the  $b\bar{b}$  final state at LEP in the same mass region. A plausible solution is that the Higgs sector is extended to include an additional Higgs boson with a mass of 95.4 GeV. We study a complex singlet scalar extension of the two-Higgs-doublet model in which the 95.4 GeV Higgs is from the mixing of three CP-even Higgs fields. In addition, the extended Higgs potential can achieve spontaneous CP-violation at the finite temperature and restore CP symmetry at the present temperature of the Universe. We find that the model can simultaneously explain the baryon asymmetry of the Universe, the diphoton and  $b\bar{b}$  excesses around the 95.4 GeV while satisfying various relevant constraints including the experiments of collider and electric dipole moment.

## I. INTRODUCTION

The baryon asymmetry of the Universe (BAU) is a fundamental question in particle physics and cosmology. By the observation based on the Big-Bang Nucleosynthesis, the BAU is [1]

$$Y_B \equiv \rho_B/s = (8.2 - 9.2) \times 10^{-11}, \quad (1)$$

where  $s$  is the entropy density, and  $\rho_B$  is the baryon number density. The three necessary Sakharov ingredients for generating such an asymmetry dynamically: baryon number violation, C and CP violations, and a departure from thermal equilibrium [2]. The electroweak baryogenesis (EWBG) [3, 4] is a promising and attractive mechanism of explaining the BAU. In order to achieve the EWBG, the SM need be extended to produce sufficient large CP-violation and a strongly first-order electroweak phase transition (PT), such as the singlet extension of SM (see for example [5–20]) and the two-Higgs-doublet model (2HDM) (see for example [21–41]).

The explicit CP-violation interactions in the lagrangian required by the EWBG can be severely constrained by the negative results in the electric dipole moment (EDM) searches for electrons [42]. The spontaneous CP-violation at finite temperature offers a valid mechanism for solving the problem. In the mechanism, no explicit CP-violating interactions are added to the lagrangian. Because of thermal corrections to the effective potential, the vacuum structure of the theory changes at finite temperature, and can dynamically induce sufficient large CP-violation to obtain the observed BAU via electroweak PT. However, as the temperature decreases, the observed electroweak vacuum is obtained and the CP symmetry is restored at the present temperature. Thus, there are no new CP-violating interactions beyond the CKM mechanism at the present temperature, and no new corrections to the EDM. As a result, the stringent EDM experimental constraints will be naturally avoided. The novel mechanism has been realized in the singlet scalar extension of the SM [14, 15] in which one need introduce a high dimension effective operator, the singlet pseudoscalar extension of 2HDM [43, 44], and the complex singlet scalar extension of 2HDM respecting a discrete dark CP symmetry in which the dark matter is simultaneously explained [45].

Based on full Run 2 data set, the CMS collaboration published the latest result of searching for low-mass diphoton, and confirmed a previously released excess at  $m_{\gamma\gamma} = 95.4$  GeV with a local significance of  $2.9\sigma$  [46]. The ATLAS collaboration also presented the result of

searching for diphoton signals in the mass range from 66 GeV to 110 GeV based on their full Run 2 dataset [47]. The ATLAS search found a diphoton excess with a local significance of  $1.7\sigma$  at the same mass value as the one that was previously reported by CMS. Neglecting possible correlations, the combined signal strength corresponds to a  $3.1\sigma$  local excess [48],

$$\mu_{\gamma\gamma}^{exp} = \mu_{\gamma\gamma}^{ATLAS+CMS} = \frac{\sigma(pp \rightarrow \phi \rightarrow \gamma\gamma)}{\sigma_{SM}(pp \rightarrow h_{95.4}^{SM} \rightarrow \gamma\gamma)} = 0.24_{-0.08}^{+0.09}, \quad (2)$$

where  $\phi$  is a non-SM scalar with a mass of 95.4 GeV, and  $h_{95.4}^{SM}$  is a hypothetical SM-like Higgs with the same mass. Interestingly, there is a longstanding  $2.3\sigma$  local excess in the  $e^+e^- \rightarrow Z(\phi \rightarrow b\bar{b})$  searches at LEP in the same mass region [49],

$$\mu_{b\bar{b}}^{exp} = 0.117 \pm 0.057. \quad (3)$$

There are numerous discussions on the excesses in the new physics models, for example Refs. [48, 50–96]. In this paper, we propose a complex singlet scalar extension of 2HDM (2HDMS) to accommodate the diphoton and  $b\bar{b}$  excesses around 95.4 GeV. Meanwhile, we discuss the spontaneous CP-violation at the finite temperature and possibility of explanation on the BAU.

The structure of this paper is outlined as follows. In Section II, we introduce some characteristic features of the 2HDMS. In Section III and IV, we discuss relevant theoretical and experimental constraints, and explain the diphoton and  $b\bar{b}$  excesses around the 95.4 GeV. In Section V and VI, we discuss the PTs of the Universe and the possibility of explaining the BAU, respectively. Finally, we draw our conclusion in Section VII.

## II. THE MODEL

The SM is augmented with a second Higgs doublet  $\Phi_2$  and a complex singlet  $S$ ,

$$\Phi_1 = \begin{pmatrix} \phi_1^+ \\ \frac{(v_1 + \rho_1 + i\eta_1)}{\sqrt{2}} \end{pmatrix}, \Phi_2 = \begin{pmatrix} \phi_2^+ \\ \frac{(v_2 + \rho_2 + i\eta_2)}{\sqrt{2}} \end{pmatrix}, S = \frac{(\rho_s + v_s + i\eta_s)}{\sqrt{2}}, \quad (4)$$

where  $v_1$ ,  $v_2$  and  $v_s$  are the real vacuum expectation values (VEVs) acquired by the fields  $\Phi_1$ ,  $\Phi_2$  and  $S$ , respectively. We define the ratio of the two VEVs as  $\tan \beta \equiv v_2/v_1$ .

The scalar potential is given by

$$\begin{aligned}
V = & m_{11}^2(\Phi_1^\dagger\Phi_1) + m_{22}^2(\Phi_2^\dagger\Phi_2) + \frac{\lambda_1}{2}(\Phi_1^\dagger\Phi_1)^2 + \frac{\lambda_2}{2}(\Phi_2^\dagger\Phi_2)^2 + \lambda_3(\Phi_1^\dagger\Phi_1)(\Phi_2^\dagger\Phi_2) \\
& + \lambda_4(\Phi_1^\dagger\Phi_2)(\Phi_2^\dagger\Phi_1) + \left[ \frac{\lambda_5}{2}(\Phi_1^\dagger\Phi_2)^2 + \lambda_6(\Phi_1^\dagger\Phi_1)(\Phi_1^\dagger\Phi_2) + \lambda_7(\Phi_2^\dagger\Phi_2)(\Phi_1^\dagger\Phi_2) + \text{h.c.} \right] \\
& + m_S^2 SS^* + \left[ \frac{m_S'^2}{2} SS + \text{h.c.} \right] + \left[ \frac{\mu_s}{6} S^3 + \frac{\mu_s'}{2} SSS^* + \text{h.c.} \right] \\
& + \left[ \frac{\lambda_1''}{24} S^4 + \frac{\lambda_2''}{6} S^2 SS^* + \text{h.c.} \right] + \frac{\lambda_3''}{4} (SS^*)^2 \\
& + SS^* \left[ \lambda_1' \Phi_1^\dagger \Phi_1 + \lambda_2' \Phi_2^\dagger \Phi_2 \right] + \left[ S^2 (\lambda_4' \Phi_1^\dagger \Phi_1 + \lambda_5' \Phi_2^\dagger \Phi_2) + \text{h.c.} \right] \\
& + \left[ (\lambda_6' SS^* + \lambda_7' SS + \lambda_8' S^* S^*) \Phi_2^\dagger \Phi_1 + \text{h.c.} \right] \\
& + \left[ -m_{12}^2 \Phi_2^\dagger \Phi_1 + \frac{\mu}{2} (S - S^*) \Phi_1^\dagger \Phi_2 + \text{h.c.} \right]. \tag{5}
\end{aligned}$$

We focus on the CP-conservation case in which all the coupling coefficients and mass are real. For simplicity, we take  $\lambda_6 = \lambda_7 = \lambda_6' = \lambda_7' = \lambda_8' = 0$  and  $\mu_s = \mu_s'$  in the following discussions. A softly-broken  $Z_2$  symmetry under which  $\Phi_1 \rightarrow \Phi_1, S \rightarrow S$  and  $\Phi_2 \rightarrow -\Phi_2$ , can be imposed to achieve  $\lambda_6 = \lambda_7 = \lambda_6' = \lambda_7' = \lambda_8' = 0$ .

The minimization conditions of the scalar potential give

$$\begin{aligned}
m_{11}^2 &= m_{12}^2 t_\beta - \frac{v^2}{2} (\lambda_1 c_\beta^2 + \lambda_{345} s_\beta^2) - \frac{v_s^2}{2} \lambda_1' - v_s^2 \lambda_4', \\
m_{22}^2 &= m_{12}^2 / t_\beta - \frac{v^2}{2} (\lambda_2 s_\beta^2 + \lambda_{345} c_\beta^2) - \frac{v_s^2}{2} \lambda_2' - v_s^2 \lambda_5', \\
m_S^2 &= -m_S'^2 - \frac{v_s^2}{12} \lambda_1'' - \frac{v_s^2}{3} \lambda_2'' - \frac{v_s^2}{4} v_s^2 \lambda_3'' - \sqrt{2} v_s \mu_s \\
&\quad - \frac{1}{2} v^2 (\lambda_1' + 2\lambda_4') c_\beta^2 - \frac{1}{2} v^2 (\lambda_2' + 2\lambda_5') s_\beta^2, \tag{6}
\end{aligned}$$

where  $t_\beta \equiv \tan \beta$ ,  $s_\beta \equiv \sin \beta$ ,  $c_\beta \equiv \cos \beta$ , and  $\lambda_{345} = \lambda_3 + \lambda_4 + \lambda_5$ .

After spontaneous symmetry breaking, the mass eigenstates are obtained from the original fields by the rotation matrices,

$$\begin{pmatrix} h_1, h_2, h_3 \end{pmatrix} = \begin{pmatrix} \rho_1, \rho_2, \rho_s \end{pmatrix} R^T, \tag{7}$$

$$\begin{pmatrix} A, X, G \end{pmatrix} = \begin{pmatrix} \eta_1, \eta_2, \eta_s \end{pmatrix} R_A^T, \tag{8}$$

$$\begin{pmatrix} G^\pm \\ H^\pm \end{pmatrix} = \begin{pmatrix} \cos \beta & \sin \beta \\ -\sin \beta & \cos \beta \end{pmatrix} \begin{pmatrix} \phi_1^\pm \\ \phi_2^\pm \end{pmatrix}, \tag{9}$$

with

$$R = \begin{pmatrix} c_1 c_2 & s_1 c_2 & s_2 \\ -s_1 c_3 - c_1 s_2 s_3 & c_1 c_3 - s_1 s_2 s_3 & c_2 s_3 \\ s_1 s_3 - c_1 s_2 c_3 & -s_1 s_2 c_3 - c_1 s_3 & c_2 c_3 \end{pmatrix}, R^A = \begin{pmatrix} -s_\beta c_4 & c_\beta c_4 & s_4 \\ s_\beta s_4 & -c_\beta s_4 & c_4 \\ c_\beta & s_\beta & 0 \end{pmatrix}. \quad (10)$$

The shorthand notations  $s_1 \equiv \sin \alpha_1$ ,  $s_2 \equiv \sin \alpha_2$ ,  $s_3 \equiv \sin \alpha_3$ , and  $s_4 \equiv \sin \alpha_4$ . The  $G^0$  and  $G^\pm$  are Goldstones, and they are absorbed by gauge bosons  $Z$  and  $W^\pm$ . The remaining physical states includes three CP-even states  $h_{1,2,3}$ , two pseudoscalars  $A$  and  $X$ , and a pair of charged scalar  $H^\pm$ .

Taking the scalar masses and mixing angles as the input parameters, one can express the coupling constants in the Higgs potential as

$$\begin{aligned} \mu &= \frac{\sqrt{2}c_4 s_4 (m_X^2 - m_A^2)}{v}, \\ \lambda_1 &= \frac{m_{h1}^2 R_{11}^2 + m_{h2}^2 R_{21}^2 + m_{h3}^2 R_{31}^2 - m_{12}^2 t_\beta}{v^2 c_\beta^2}, \\ \lambda_2 &= \frac{m_{h1}^2 R_{12}^2 + m_{h2}^2 R_{22}^2 + m_{h3}^2 R_{32}^2 - m_{12}^2 t_\beta^{-1}}{v^2 s_\beta^2}, \\ \lambda_3 &= \frac{m_{h1}^2 R_{11} R_{12} + m_{h2}^2 R_{21} R_{22} + m_{h3}^2 R_{31} R_{32} + 2m_{H^\pm}^2 s_\beta c_\beta - m_{12}^2}{v^2 s_\beta c_\beta}, \\ \lambda_4 &= \frac{(m_A^2 c_4^2 + m_X^2 s_4^2 - 2m_{H^\pm}^2) s_\beta c_\beta + m_{12}^2}{v^2 s_\beta c_\beta}, \\ \lambda_5 &= \frac{-(m_A^2 c_4^2 + m_X^2 s_4^2) s_\beta c_\beta + m_{12}^2}{v^2 s_\beta c_\beta}, \\ \lambda'_4 &= -\frac{3c_4^2 m_X^2 + 6m_S'^2 + 3m_A^2 s_4^2 + 6\lambda_5' s_\beta^2 v^2 + 3\sqrt{2}\mu_s v_s + (\lambda_1'' + \lambda_2'')v_s^2}{6v^2 c_\beta^2}, \\ \lambda'_1 &= -2\lambda'_4 + \frac{(m_{h1}^2 R_{11} R_{13} + m_{h2}^2 R_{21} R_{23} + m_{h3}^2 R_{31} R_{33})}{vv_s c_\beta}, \\ \lambda'_2 &= -2\lambda'_5 + \frac{(m_{h1}^2 R_{12} R_{13} + m_{h2}^2 R_{22} R_{23} + m_{h3}^2 R_{32} R_{33})}{vv_s s_\beta}, \\ \lambda_3'' &= \frac{6m_{h1}^2 R_{13}^2 + 6m_{h2}^2 R_{23}^2 + 6m_{h3}^2 R_{33}^2 - v_s(6\sqrt{2}\mu_s + \lambda_1'' v_s + 4\lambda_2'' v_s)}{3v_s^2}. \end{aligned} \quad (11)$$

The general Yukawa interactions are written as

$$\begin{aligned} -\mathcal{L} &= Y_{u2} \bar{Q}_L \tilde{\Phi}_2 u_R + Y_{d2} \bar{Q}_L \Phi_2 d_R + Y_{\ell 2} \bar{L}_L \Phi_2 e_R \\ &+ Y_{u1} \bar{Q}_L \tilde{\Phi}_1 u_R + Y_{d1} \bar{Q}_L \Phi_1 d_R + Y_{\ell 1} \bar{L}_L \Phi_1 e_R + \text{h.c.}, \end{aligned} \quad (12)$$

where  $Q_L^T = (u_L, d_L)$ ,  $L_L^T = (\nu_L, l_L)$ ,  $\tilde{\Phi}_{1,2} = i\tau_2 \Phi_{1,2}^*$ , and  $Y_{u1,2}$ ,  $Y_{d1,2}$  and  $Y_{\ell1,2}$  are  $3 \times 3$  matrices in family space. We assume the Yukawa coupling matrices to be aligned to avoid the tree-level flavour changing neutral current [97, 98],

$$\begin{aligned} (Y_{u1})_{ii} &= \frac{\sqrt{2}m_{ui}}{v}\rho_{1u}, & (Y_{u2})_{ii} &= \frac{\sqrt{2}m_{ui}}{v}\rho_{2u}, \\ (Y_{\ell1})_{ii} &= \frac{\sqrt{2}m_{\ell i}}{v}\rho_{1\ell}, & (Y_{\ell2})_{ii} &= \frac{\sqrt{2}m_{\ell i}}{v}\rho_{2\ell}, \\ (X_{d1})_{ii} &= \frac{\sqrt{2}m_{di}}{v}\rho_{1d}, & (X_{d2})_{ii} &= \frac{\sqrt{2}m_{di}}{v}\rho_{2d}, \end{aligned} \quad (13)$$

where all the off-diagonal elements are zero, and  $\rho_{1f} = (c_\beta - s_\beta \kappa_f)$  and  $\rho_{2f} = (s_\beta + c_\beta \kappa_f)$  with  $f = u, d, \ell$ .  $\kappa_f$  are new free parameters, which determine the Yukawa coupling matrices of up-type quark, down-type quark, and lepton.  $X_{d1,2} = V_{dL}^\dagger Y_{d1,2} V_{dR}$  with  $V_{dL} \equiv V_{CKM}$ , where  $V_{dL,R}$  are unitary matrices which transform the interaction eigenstates to the mass eigenstates for the left-handed and right-handed down-type quark fields. The Yukawa interactions will explicitly break the  $Z_2$  symmetry mentioned above.

The couplings of the neutral Higgs bosons with respect to the SM are given by

$$\begin{aligned} y_V^{h_1} &= c_2 c_{\beta 1}, \quad y_f^{h_1} = c_2 (c_{\beta 1} - s_{\beta 1} \kappa_f), \\ y_V^{h_2} &\simeq |s_2| s_{\beta 13} + \frac{c_2^2}{2} c_3 s_{\beta 1}, \quad y_f^{h_2} \simeq |s_2| (s_{\beta 13} + c_{\beta 13} \kappa_f) + \frac{c_2^2}{2} c_3 (s_{\beta 1} + c_{\beta 1} \kappa_f), \\ y_V^{h_3} &\simeq |s_2| c_{\beta 13} - \frac{c_2^2}{2} c_3 s_{\beta 1}, \quad y_f^{h_3} \simeq |s_2| (c_{\beta 13} - s_{\beta 13} \kappa_f) - \frac{c_2^2}{2} c_3 (s_{\beta 1} + c_{\beta 1} \kappa_f), \\ y_V^A &= 0, \quad y_A^f = -i\kappa_f \text{ (for } u) c_4, \quad y_f^A = i\kappa_f c_4 \text{ (for } d, \ell), \\ y_V^X &= 0, \quad y_X^f = i\kappa_f \text{ (for } u) s_4, \quad y_f^X = -i\kappa_f s_4 \text{ (for } d, \ell), \end{aligned} \quad (14)$$

where  $V$  denotes  $Z$  or  $W$ . The shorthand notations  $c_{\beta 1} \equiv \cos(\beta - \alpha_1)$ ,  $s_{\beta 1} \equiv \sin(\beta - \alpha_1)$ ,  $c_{\beta 13} \equiv \cos(\beta - \alpha_1 - \text{sgn}(s_2)\alpha_3)$ , and  $s_{\beta 13} \equiv \sin(\beta - \alpha_1 - \text{sgn}(s_2)\alpha_3)$ . We take the approximation of  $s_2 \simeq \text{sgn}(s_2)(1 - \frac{c_2^2}{2})$  for the expressions in the second and third lines of Eq. (14)

The Yukawa couplings of the charged Higgs are

$$\mathcal{L}_Y = -\frac{\sqrt{2}}{v} H^+ \left\{ \bar{u}_i [\kappa_d (V_{CKM})_{ij} m_{dj} P_R - \kappa_u m_{ui} (V_{CKM})_{ij} P_L] d_j + \kappa_\ell \bar{\nu} m_\ell P_R \ell \right\} + h.c., \quad (15)$$

where  $i, j = 1, 2, 3$  are the index of generation.

### III. RELEVANT THEORETICAL AND EXPERIMENTAL CONSTRAINTS

In our calculations, we consider the following theoretical and experimental constraints:

**(1) The signal data of the 125 GeV Higgs.** We take  $h_2$  as the observed 125 GeV state, and apply **HiggsTools** [99] to calculate the total  $\chi^2$  of the latest LHC rate measurements of the observed Higgs boson at 125 GeV. **HiggsTools** incorporates the codes **HiggsSignals** [99, 100] and **HiggsBounds** [101, 102]. We pay particular attention to the surviving samples with  $\chi^2 - \chi_{SM}^2 < 6.18$ , where  $\chi_{SM}^2$  denotes the  $\chi^2$  value of the SM. These samples are favoured compared to the SM fit result within  $2\sigma$  confidence level (assuming two-dimensional parameter estimations).

**(2) The searches for extra Higgses at the collider and the flavor observables.** We employ **Higgstools** to pick out the samples which meet the 95% confidence level exclusion limits from searches for the additional Higgs at the collider. **SuperIso-v4.1** [103] is used to check the compatibility with  $B \rightarrow X_s \gamma$  transitions

**(3) Vacuum stability.** We impose the conditions that the vacuum should be a global minimum of the potential, and the potential remains positive when the field values approach infinity, namely boundedness from below. For large values of the fields, the quadratic and cubic terms can be neglected, and the quartic part  $V_{4-min}$  in Eq. (5) is written in matrix form in the basis  $B = \left( \Phi_1^\dagger \Phi_1, \Phi_2^\dagger \Phi_2, \rho_S^2, \eta_S^2 \right)^T$ ,

$$\begin{aligned}
 V_{4-min} &= C^T \frac{1}{2} \underbrace{\begin{pmatrix} \lambda_1 & \lambda_3 + \Delta & \lambda'_1 + 2\lambda'_4 & \lambda'_1 - 2\lambda'_4 \\ \lambda_3 + \Delta & \lambda_2 & \lambda'_2 + 2\lambda'_5 & \lambda'_2 - 2\lambda'_5 \\ \lambda'_1 + 2\lambda'_4 & \lambda'_2 + 2\lambda'_5 & \frac{\lambda''_1 + 3\lambda''_3 + 4\lambda''_2}{6} & \frac{-\lambda''_1 + \lambda''_3}{2} \\ \lambda'_1 - 2\lambda'_4 & \lambda'_2 - 2\lambda'_5 & \frac{-\lambda''_1 + \lambda''_3}{2} & \frac{\lambda''_1 + 3\lambda''_3 - 4\lambda''_2}{6} \end{pmatrix}}_A C \\
 &= \frac{1}{2} C^T A C,
 \end{aligned} \tag{16}$$

with  $\Delta = 0$  for  $\lambda_4 \geq |\lambda_5|$  and  $\Delta = \lambda_4 - |\lambda_5|$  for  $\lambda_4 < |\lambda_5|$ . Boundedness from below demands  $A$  is a copositive matrix. Deleting the  $i$ -th row and column of  $A$ ,  $i = 1, 2, 3, 4$ , and four symmetric  $3 \times 3$  matrices are remained. The copositivity of the symmetric order 3 matrix

$B$  with entries  $b_{ij}$ ,  $i, j = 1, 2, 3$  demands [75, 104]

$$\begin{aligned}
b_{11} &\geq 0, & b_{22} &\geq 0, & b_{33} &\geq 0, \\
\bar{b}_{12} &= b_{12} + \sqrt{b_{11}b_{22}} \geq 0, \\
\bar{b}_{13} &= b_{13} + \sqrt{b_{11}b_{33}} \geq 0, \\
\bar{b}_{23} &= b_{23} + \sqrt{b_{22}b_{33}} \geq 0, \\
\sqrt{b_{11}b_{22}b_{33}} + b_{12}\sqrt{b_{33}} + b_{13}\sqrt{b_{22}} + b_{23}\sqrt{b_{11}} + \sqrt{2\bar{b}_{12}\bar{b}_{13}\bar{b}_{23}} &\geq 0.
\end{aligned} \tag{17}$$

Besides, the copositivity of matrix  $A$  requires  $\det(A) \geq 0 \vee (\text{adj}A)_{ij} < 0$ , for some  $i, j$ . The adjugate of  $A$  is the transpose of the cofactor matrix of  $A$ ,  $(\text{adj}A)_{ij} = (-1)^{i+j}M_{ji}$ . The  $M_{ij}$  is the determinant of the submatrix which is obtained by deleting row  $i$  and column  $j$  of  $A$ .

**(4) Tree-level perturbative unitarity.** We require that the eigenvalues of the  $2 \rightarrow 2$  scalar-scalar scattering matrix are below  $8\pi$ , which is achieved in **SPheno-v4.0.5** [105] employing **SARAH-SPheno** files [106].

**(5) The oblique parameters.** The oblique parameters can impose constraints on the Higgs mass spectrum in the model. For points being in agreement with the experimental observation, it was required that the values of the  $S$  and the  $T$  parameter are within the  $2\sigma$  ranges, corresponding to  $\chi^2 = 6.18$  for two degrees of freedom. The fit results are given in Ref. [1],

$$S = 0.00 \pm 0.07, \quad T = 0.05 \pm 0.06, \tag{18}$$

with the correlation coefficients,  $\rho_{ST} = 0.92$ .



In the model, the  $S$  and  $T$  are approximately calculated by [107, 108]

$$\begin{aligned}
S &= \frac{1}{\pi m_Z^2} \left[ \sum_{i=1,2,3} (F_S(m_Z^2, m_{h_i}^2, m_A^2)(R_{11}^A R_{i1} + R_{12}^A R_{i2})^2 \right. \\
&\quad + F_S(m_Z^2, m_{h_i}^2, m_X^2)(R_{21}^A R_{i1} + R_{22}^A R_{i2})^2 + F_S(m_Z^2, m_Z^2, m_{h_i}^2)(c_\beta R_{i1} + s_\beta R_{i2})^2 \\
&\quad - m_Z^2 F_{S0}(m_Z^2, m_Z^2, m_{h_i}^2)(c_\beta R_{i1} + s_\beta R_{i2})^2) \\
&\quad \left. - F_S(m_Z^2, m_{H^\pm}^2, m_{H^\pm}^2) - F_S(m_Z^2, m_Z^2, m_{ref}^2) + m_Z^2 F_{S0}(m_Z^2, m_Z^2, m_{ref}^2) \right], \\
T &= \frac{1}{16\pi m_W^2 s_W^2} \left[ \sum_{i=1,2,3} (-F_T(m_{h_i}^2, m_A^2)(R_{11}^A R_{i1} + R_{12}^A R_{i2})^2 \right. \\
&\quad - F_T(m_{h_i}^2, m_X^2)(R_{21}^A R_{i1} + R_{22}^A R_{i2})^2 + F_T(m_{H^\pm}^2, m_{h_i}^2)(c_\beta R_{i2} - s_\beta R_{i1})^2 \\
&\quad + 3F_T(m_Z^2, m_{h_i}^2)(c_\beta R_{i1} + s_\beta R_{i2})^2 - 3F_T(m_W^2, m_{h_i}^2)(c_\beta R_{i1} + s_\beta R_{i2})^2) \\
&\quad + F_T(m_{H^\pm}^2, m_A^2)(c_\beta R_{12}^A - s_\beta R_{11}^A)^2 + F_T(m_{H^\pm}^2, m_X^2)(c_\beta R_{22}^A - s_\beta R_{21}^A)^2 \\
&\quad \left. - 3F_T(m_Z^2, m_{ref}^2) + 3F_T(m_W^2, m_{ref}^2) \right], \tag{19}
\end{aligned}$$

where

$$\begin{aligned}
F_T(a, b) &= \frac{1}{2}(a + b) - \frac{ab}{a - b} \log\left(\frac{a}{b}\right), \quad F_S(a, b, c) = B_{22}(a, b, c) - B_{22}(0, b, c), \\
F_{S0}(a, b, c) &= B_0(a, b, c) - B_0(0, b, c) \tag{20}
\end{aligned}$$

with

$$\begin{aligned}
B_{22}(a, b, c) &= \frac{1}{4} \left[ b + c - \frac{1}{3}a \right] - \frac{1}{2} \int_0^1 dx \, X \log(X - i\epsilon), \\
B_0(a, b, c) &= - \int_0^1 dx \, \log(X - i\epsilon), \\
X &= bx + c(1 - x) - ax(1 - x). \tag{21}
\end{aligned}$$

#### IV. EXCESSES AROUND 95.4 GEV

The assumed origins of the diphoton and  $b\bar{b}$  excesses around the 95.4 GeV are the resonant productions of the lightest CP-even Higgs  $h_1$  in the model. In the narrow width approximation, these signal strengths can be expressed as follows:

$$\mu_{b\bar{b}} = \frac{\sigma_{2\text{HDMS}}(e^+e^- \rightarrow Zh_1)}{\sigma_{\text{SM}}(e^+e^- \rightarrow Zh_{95.4}^{\text{SM}})} \times \frac{\text{BR}_{2\text{HDMS}}(h_1 \rightarrow b\bar{b})}{\text{BR}_{\text{SM}}(h_{95.4}^{\text{SM}} \rightarrow b\bar{b})} = |y_V^{h_1}|^2 \frac{\text{BR}_{2\text{HDMS}}(h_1 \rightarrow b\bar{b})}{\text{BR}_{\text{SM}}(h_{95.4}^{\text{SM}} \rightarrow b\bar{b})} \tag{22}$$

$$\mu_{\gamma\gamma} = \frac{\sigma_{2\text{HDMS}}(gg \rightarrow h_1)}{\sigma_{\text{SM}}(gg \rightarrow h_{95.4}^{\text{SM}})} \times \frac{\text{BR}_{2\text{HDMS}}(h_1 \rightarrow \gamma\gamma)}{\text{BR}_{\text{SM}}(h_{95.4}^{\text{SM}} \rightarrow \gamma\gamma)} \simeq |y_u^{h_1}|^2 \frac{\text{BR}_{2\text{HDMS}}(h_1 \rightarrow \gamma\gamma)}{\text{BR}_{\text{SM}}(h_{95.4}^{\text{SM}} \rightarrow \gamma\gamma)} \tag{23}$$

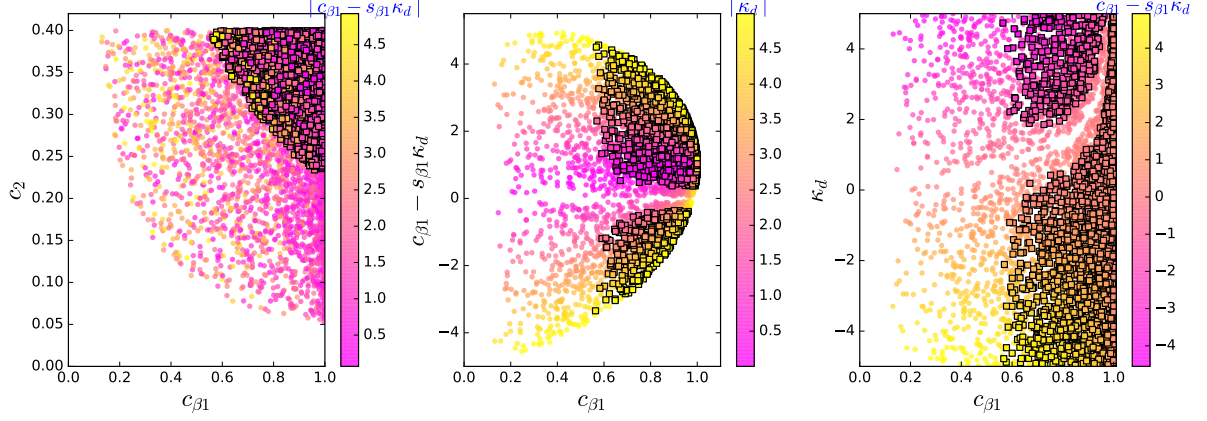


FIG. 1: The samples accommodating the  $b\bar{b}$  excess at the 95.4 GeV. The excess is explained within  $1\sigma$  and  $2\sigma$  ranges for the squares and circles, respectively.

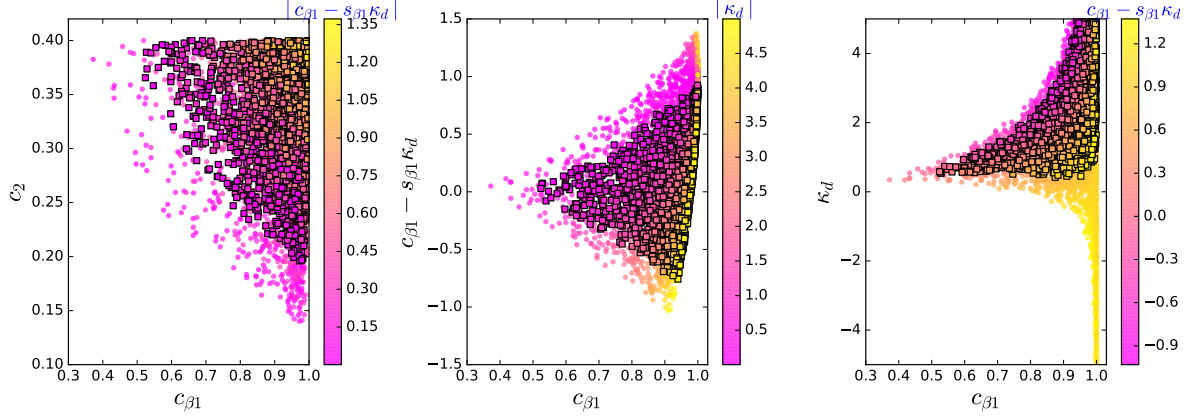


FIG. 2: Same as the Fig. 1, but for the diphoton excess at the 95.4 GeV.

In our calculations, we take the mixing parameters and Yukawa parameters as follows:

$$\begin{aligned}
0 \leq c_2 \leq 0.4, \quad s_{\beta 13} = 1.0, \quad 0.5 \leq \tan \beta \leq 2, \\
0 \leq s_{\beta 1} \leq 1.0, \quad 0.2 \leq s_4 \leq 0.7, \\
\kappa_u = 0, \quad \kappa_\ell = 0, \quad -5.0 \leq \kappa_d \leq 5.0.
\end{aligned} \tag{24}$$

For  $s_{\beta 13} = 1.0$  and  $c_2 \rightarrow 0$ , the couplings between the  $h_2$  and SM particles approach to those of SM, which is favored by the signal data of the 125 GeV Higgs. In order to weaken the bounds on the extra Higgses from the direct searches at the LHC and indirect searches via the flavour physics data, we choose  $\kappa_u = \kappa_\ell = 0$  and  $-5.0 \leq \kappa_d \leq 5.0$ . The nonzero  $\kappa_d$  can make  $y_d^{h_1}$  to be smaller than  $y_V^{h_1}$  and  $y_u^{h_1}$ , and suppress the total width of  $h_1$  significantly. As a result,  $Br(h_1 \rightarrow \gamma\gamma)$  is sizably enhanced.

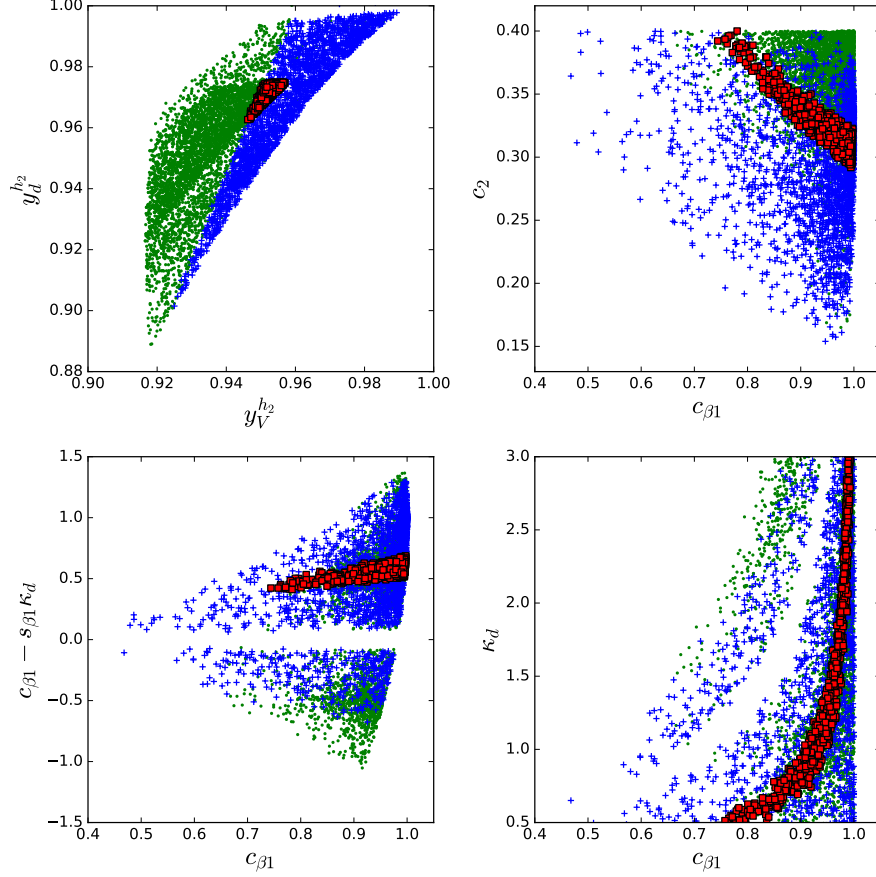


FIG. 3: The circles (green) are excluded by the constraints of "pre-95" while the pluses (blue) and squares (red) are allowed. The  $b\bar{b}$  and diphoton excesses are simultaneously explained within  $1\sigma$  and  $2\sigma$  ranges for squares (red) and the pluses (blue).

In Fig. 1 and Fig. 2 we respectively display the parameter points explaining the  $b\bar{b}$  and diphoton excesses at the 95.4 GeV within  $1\sigma$  and  $2\sigma$  ranges without imposing any other constraints. From Fig. 1, it can be observed that  $c_2$  is imposed a lower bound for a given  $c_{\beta 1}$  since the signal strength  $\mu_{b\bar{b}}$  is directly proportional to  $|y_{h_1}^V|^2$ . The Yukawa coupling of bottom quark to  $h_1$  is proportional to  $c_{\beta 1} - s_{\beta 1}\kappa_d$ , and therefore a relative large value of  $|c_{\beta 1} - s_{\beta 1}\kappa_d|$  is favored to explain the  $b\bar{b}$  excess, especially for the explanation within  $1\sigma$  range. The allowed  $\kappa_d$  and  $c_{\beta 1}$  are displayed in the right panel of Fig. 1. Different from the case of the  $b\bar{b}$  excess, the explanation of diphoton excess at the 95.4 GeV favors a relative small  $|c_{\beta 1} - s_{\beta 1}\kappa_d|$ , which can suppress the total width of  $h_1$ , and then enhance  $Br(h_1 \rightarrow \gamma\gamma)$ . As a result, a positive  $\kappa_d$  is favored for the case of  $c_{\beta 1} > 0$  and  $s_{\beta 1} > 0$ . When  $c_{\beta 1}$  approaches to 1.0, a negative  $\kappa_d$  is allowed to explain the diphoton excess with  $2\sigma$  range, as shown in

the right panel of Fig. 2.

After imposing the constraints of "pre-95" (denoting theoretical constraints, the oblique parameters, the signal data of the 125 GeV Higgs, the searches for extra Higgses at the LHC and the flavor observables), we show the parameter points explaining the diphoton and  $b\bar{b}$  excesses at the 95.4 GeV in Fig. 3. We find that the whole parameter space chosen in the Eq. (24) can be consistent with the measurement of  $B \rightarrow X_s \gamma$ . The choice of  $\kappa_u = 0$  can suppress the top Yukawa couplings to  $H$ ,  $A$ ,  $X$ , and  $H^\pm$ , and reduce the production cross sections of these extra Higgses at the LHC. As a result, the exclusion bounds of searches for additional Higgs bosons at the LHC can be markedly weakened. The signal data of the 125 GeV Higgs impose stringent constraints on  $y_V^{h_2}$  and  $y_d^{h_2}$ , and exclude many parameter points explaining the  $b\bar{b}$  and diphoton excesses. In the region of  $0.15 < c_2 < 0.4$  and  $0.45 < c_{\beta 1} < 1.0$ , the model can simultaneously explain the  $b\bar{b}$  and diphoton excesses at the 95.4 GeV within  $2\sigma$  ranges. The  $|\kappa_d|$  is favored to decrease with  $c_{\beta 1}$ , and  $0 < \kappa_d < 1$  is required for the case of  $c_{\beta 1} < 0.6$ . There is a small region explaining both  $b\bar{b}$  and diphoton excesses within  $1\sigma$  range, in which  $c_2$ ,  $c_{\beta 1}$ , and  $\kappa_d$  have strong dependencies.

## V. PHASE TRANSITION

To examine the PTs we first study the effective scalar potential of the model at finite temperature. The neutral elements of  $\Phi_1$  and  $\Phi_2$  are parametrized as  $\frac{\varphi_1}{\sqrt{2}}$  and  $\frac{\varphi_2 + i\varphi_3}{\sqrt{2}}$ , and the singlet scalar field is parametrized as  $\frac{\chi + i\eta_s}{\sqrt{2}}$ . It is plausible to choose the imaginary part of the neutral component of  $\Phi_1$  to be zero because the potential of Eq. (5) only depends on the relative phase of the neutral components of  $\Phi_1$  and  $\Phi_2$ .

The full effective potential at finite temperature is gauge-dependent [109, 110], which is composed of four parts: the tree level potential, the Coleman-Weinberg term [111], the finite temperature corrections [112] and the resummed daisy corrections [113, 114]. In this paper we consider the high-temperature approximation of effective potential, which keeps only the tree-level potential and the thermal mass terms in the high-temperature expansion. Therefore, the effective potential is gauge invariant, and it does not depend on the resummation scheme and the renormalization scheme. The high-temperature approximation of effective

potential is written as

$$\begin{aligned}
V_{eff}(\varphi_1, \varphi_2, \varphi_3, \chi, \eta_s) = & \frac{1}{2}(m_{11}^2 + \Pi_{\varphi_1})\varphi_1^2 + \frac{1}{2}(m_{22}^2 + \Pi_{\varphi_2})(\varphi_2^2 + \varphi_3^2) + \frac{1}{2}(m_S^2 + m_S'^2 + \Pi_\chi)\chi^2 \\
& + \frac{1}{2}(m_S^2 - m_S'^2 + \Pi_{\eta_s})\eta_s^2 + \frac{1}{8}(\lambda_1\varphi_1^4 + \lambda_2\varphi_2^4 + \lambda_3\varphi_3^4) + \frac{1}{4}\lambda_{345}\varphi_1^2\varphi_2^2 + \frac{1}{4}\bar{\lambda}_{345}\varphi_1^2\varphi_3^2 \\
& + \frac{\lambda_2}{4}\varphi_3^2\varphi_2^2 - m_{12}^2\varphi_1\varphi_2 - \frac{\mu}{\sqrt{2}}\varphi_3\eta_s\varphi_1 + \frac{\lambda_1'}{4}(\chi^2 + \eta_s^2)\varphi_1^2 + \frac{\lambda_2'}{4}(\chi^2 + \eta_s^2)(\varphi_2^2 + \varphi_3^2) \\
& + \frac{\lambda_4'}{2}(\chi^2 - \eta_s^2)\varphi_1^2 + \frac{\lambda_5'}{2}(\chi^2 - \eta_s^2)(\varphi_3^2 + \varphi_2^2) + (\frac{\lambda_1''}{48} + \frac{\lambda_3''}{16})(\chi^4 + \eta_s^4) + \frac{1}{8}(\lambda_3'' - \lambda_1'')\chi^2\eta_s^2 \\
& + \frac{\lambda_2''}{12}(\chi^4 - \eta_s^4) + \frac{\sqrt{2}}{3}\mu_s\chi^3, \\
\Pi_{\varphi_1} = & \left[ \frac{9g^2}{2} + \frac{3g'^2}{2} + 6\lambda_1 + 4\lambda_3 + 2\lambda_4 + 2\lambda_1' + 6y_t^2(c_\beta - s_\beta\kappa_u)^2 + 6y_b^2(c_\beta - s_\beta\kappa_d)^2 \right] \frac{T^2}{24}, \\
\Pi_{\varphi_2} = & \left[ \frac{9g^2}{2} + \frac{3g'^2}{2} + 6\lambda_2 + 4\lambda_3 + 2\lambda_4 + 2\lambda_2' + 6y_t^2(s_\beta + c_\beta\kappa_u)^2 + 6y_b^2(s_\beta + c_\beta\kappa_d)^2 \right] \frac{T^2}{24}, \\
\Pi_{\varphi_3} = & \Pi_{\varphi_2}, \\
\Pi_\chi = & [4\lambda_1' + 4\lambda_2' + 2\lambda_2'' + 2\lambda_3'' + 8\lambda_4' + 8\lambda_5'] \frac{T^2}{24}, \\
\Pi_{\eta_s} = & [4\lambda_1' + 4\lambda_2' - 2\lambda_2'' + 2\lambda_3'' - 8\lambda_4' - 8\lambda_5'] \frac{T^2}{24}, \tag{25}
\end{aligned}$$

where  $\bar{\lambda}_{345} = \lambda_3 + \lambda_4 - \lambda_5$ ,  $y_t = \frac{\sqrt{2}m_t}{v}$ ,  $y_b = \frac{\sqrt{2}m_b}{v}$ , and  $\Pi_i$  denotes the thermal mass terms of the field  $i$ .

In a first-order PT, the bubble nucleation rate per unit volume at the finite temperature is given by [115–117]

$$\Gamma \approx A(T)e^{-S_3/T}, \tag{26}$$

where  $A(T) \sim T^4$  is a prefactor and  $S_3$  is a three-dimensional Euclidian action,

$$S_3 = 4\pi \int_0^\infty dr r^2 \left[ \sum_{i=1}^5 \frac{1}{2} \left( \frac{d\phi_i}{dr} \right)^2 + V_{eff} \right]. \tag{27}$$

The  $\phi_{i=1,2,3,4,5}$  denotes  $\varphi_1, \varphi_2, \varphi_3, \chi$ , and  $\eta_s$ , which are determined by bounce equations [118]

$$\frac{d^2\phi_i}{dr^2} + \frac{2}{r} \frac{d\phi_i}{dr} = \frac{\partial V_{eff}}{\partial \phi_i}, \quad (i = 1, 2, 3, 4, 5). \tag{28}$$

We employ **FindBounce** to solve the bounce equations, and obtain the bubble wall VEV profiles [119]. At the nucleation temperature  $T_n$ , the thermal tunneling probability for bubble nucleation per horizon volume and per horizon time is of order one, and this condition is roughly converted to the relation  $\frac{S_3(T)}{T}|_{T=T_n} \approx 140$ .

	$m_{h_1}(\text{GeV})$	$m_{h_2}(\text{GeV})$	$m_{h_3} = m_{H^\pm}(\text{GeV})$	$m_A(\text{GeV})$	$m_X(\text{GeV})$	$m_{12}^2(\text{GeV})^2$	$m_s'^2(\text{GeV})^2$
BP1	95.4	125.0	451.42	80.99	412.39	5314.36	4720.09
BP2	95.4	125.0	570.22	70.40	275.10	2482.07	5067.11

	$t_\beta$	$s_{\beta 13}$	$c_2$	$s_{\beta 1}$	$s_4$	$\lambda'_5$	$\lambda''_1$	$\lambda''_2$	$\kappa_d$	$\kappa_u = \kappa_\ell$	$\mu_s(\text{GeV})$	$v_s(\text{GeV})$	$\mu_{b\bar{b}}$	$\mu_{\gamma\gamma}$
BP1	1.147	1.0	0.277	0.382	0.317	-1.429	3.908	3.166	0.954	0.0	73.48	-50.11	0.0489	0.118
BP2	0.950	1.0	0.247	0.498	0.426	-1.024	4.384	2.324	0.891	0.0	101.63	-67.05	0.0280	0.104

TABLE I: Input parameters for the BP1 and the BP2.

The CP symmetry is conserved both at very high temperature and the present temperature, and it is only spontaneously broken at the finite temperature. Therefore, the Universe need undergo multi-step PTs. It is noted that the effective potential  $V_{eff}$  in Eq. (25) has a  $Z_2$  symmetry:  $\varphi_3 \rightarrow -\varphi_3$  and  $\eta_s \rightarrow -\eta_s$ . Therefore, there will not be a bias between transitions to  $(\langle\varphi_1\rangle, \langle\varphi_2\rangle, \langle\varphi_3\rangle, \langle\chi\rangle, \langle\eta_s\rangle)$  and  $(\langle\varphi_1\rangle, \langle\varphi_2\rangle, -\langle\varphi_3\rangle, \langle\chi\rangle, -\langle\eta_s\rangle)$  from the origin  $(0, 0, 0, 0, 0)$  GeV. The two kinds of bubbles will create baryon asymmetry of opposite signs. As a result, the net BAU averaged over the entire Universe will be zero resulting in a null BAU. The issue can be solved in a special pattern of three-step PTs. The first step is the  $Z_2$ -breaking PT, and the second step is a strongly first-order electroweak PT during which the BAU is generated. Finally, through the third-step PT the observed vacuum is obtained and the CP symmetry is recovered at the present temperature. During the first  $Z_2$ -breaking PT, different patches of the Universe would end up in either  $+\langle\eta_s\rangle$  or  $-\langle\eta_s\rangle$  vacuum, forming a network of domains. One may add a  $Z_2$  symmetry breaking term,  $-i\mu_3(S - S^*)^3$ , which leads to a potential difference between the vacua with  $\pm\langle\eta_s\rangle$ ,  $\Delta V$ . The amount of bias  $\Delta V$  needed for the deeper minimum to be the only vacuum remaining when the next electroweak PT transition happens is very tiny,  $\Delta V/T^4 > 10^{-16}$  [5, 120]. Despite the  $\mu_3$  term breaks the CP symmetry explicitly, the CP-conservation is still a safe approximation in the model because of a negligible value of  $\mu_3$ .

We apply **CosmoTransitions** to analyze the PTs [121]. After imposing the constraints of "pre-95" and requirement of explaining both  $b\bar{b}$  and diphoton excesses within  $2\sigma$  ranges, we find two different patterns of the three-step PTs with the characteristics mentioned above, and take two benchmark points BP1 and BP2 to discuss the PTs detailedly. The key input parameters are displayed in Table I. Fig. 4 and Fig. 5 exhibit the phase histories for the

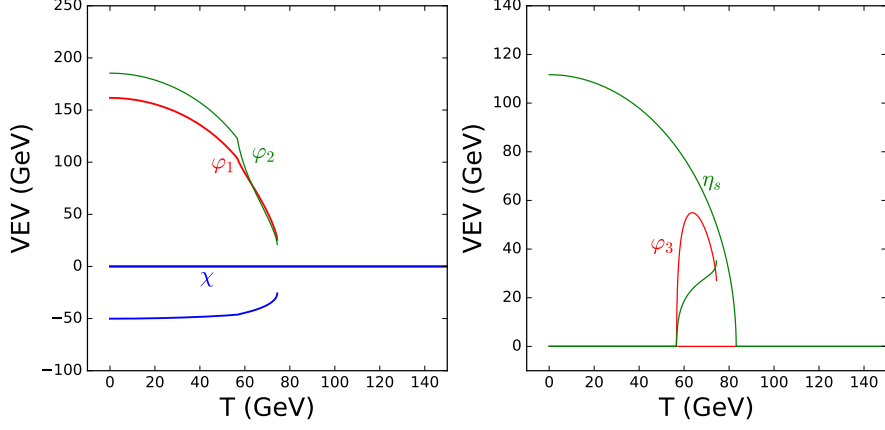


FIG. 4: Phase histories for the BP1.  $\phi(i)$  denotes the VEV of  $\phi$  at the  $i$ -th phase, where  $\phi = \varphi_1, \varphi_2, \chi, \varphi_3, \eta_s$ . The black dot represents the occurrence of a second-order PT.

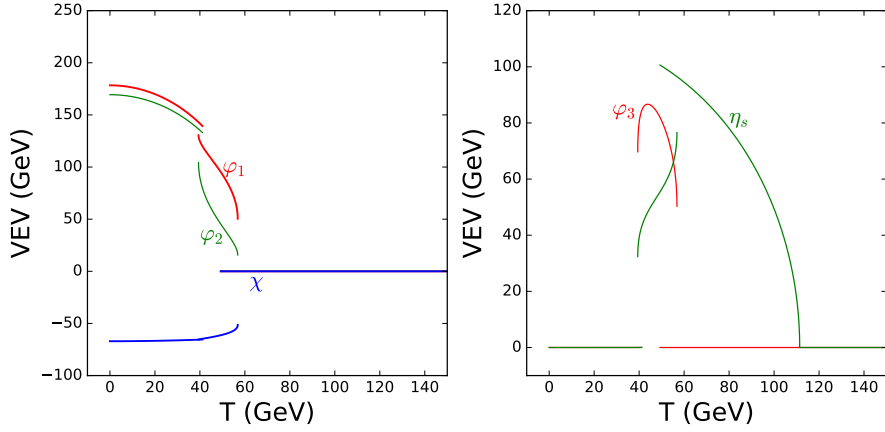


FIG. 5: Same as Fig. 1, but for the BP2.

BP1 and BP2. For the BP1, at a very high temperature, the minimum of the potential is at the origin since the contributions of the thermal mass terms to the effective potential are proportional to  $T^2$ . When the temperature decreases to  $T=83.15$  GeV, a second-order PT starts during which  $\eta_s$  develops a nonzero VEV and the other four fields still remain zero. At  $T=65.81$  GeV, a strongly first-order electroweak PT happens which breaks electroweak symmetry,  $(0, 0, 0, 0, 68.27)$  GeV  $\rightarrow (68.88, 66.0, 53.86, -40.83, 25.47)$  GeV for  $(\langle\varphi_1\rangle, \langle\varphi_2\rangle, \langle\varphi_3\rangle, \langle\chi\rangle, \langle\eta_s\rangle)$ . The strength of PT ( $\xi = \frac{\sqrt{\varphi_1^2 + \varphi_2^2 + \varphi_3^2}}{T}$ ) is 1.66, and the BAU is generated via the EWBG mechanism. At  $T=56.59$  GeV, another second-order PT takes place. Next, the vacuum evolves along the final phase, and ultimately ends in the observed values at  $T = 0$  GeV while the CP symmetry is restored. Meanwhile,  $\xi > 1$  is always remained so that the

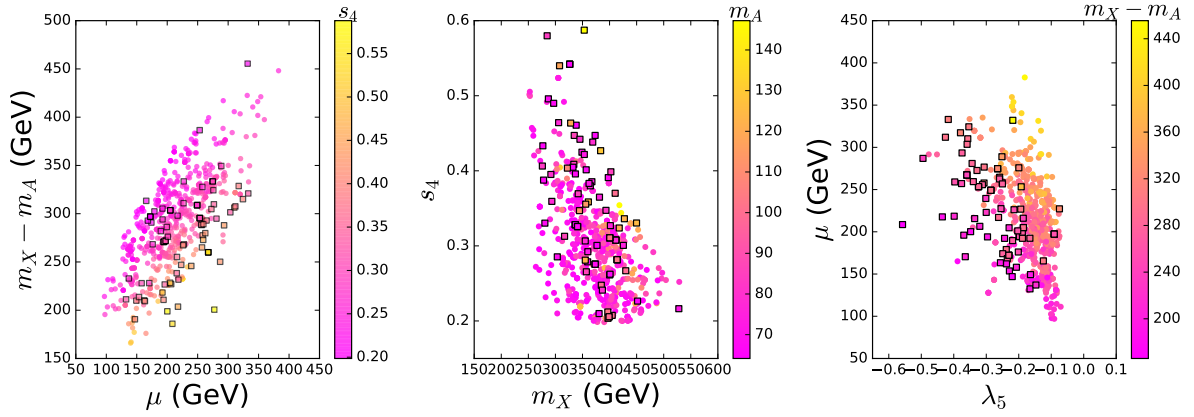


FIG. 6: The scattering plots achieving the three-step PTs with the characteristics mentioned in the text. The third step is respectively first-order PT and second-order PT for the squares and circles.

BAU is not washed out by the sphaleron process [122].

For the BP2, the first step is second-order PT and the second step is strongly first-order PT, which are similar to those of BP1. However, the third step is first-order PT during which the observed vacuum is obtained and the CP symmetry is restored.

There are no explicit CP-violating interactions in the scalar potential in Eq. (5). Due to the thermal corrections to the effective potential in Eq. (25), the  $\eta_s$  field firstly acquires a nonzero VEV at finite temperature. Naturally, the mass term and interaction terms of the  $S$  field will play an important role. In addition, the  $\mu$  term (see Eq. (5) and Eq. (25)) can lead to a close correlation between  $\langle\varphi_3\rangle$  and  $\langle\eta_s\rangle$  of the potential minimum, which plays a key role in the  $\varphi_3$  field acquiring a nonzero VEV as the temperature evolves. Thus, an imaginary part of the top quark mass is induced by the interaction of  $t\bar{t}(\varphi_2 + i\varphi_3)$ .

In Fig. 6 we display some parameter points achieving the three-step PTs. From Fig. 6, we find that the three-step PTs satisfying our requirements favor an appropriate value of  $\mu$ . As a result, according to Eq. (11),  $m_A$  and  $m_X$  is required to have a large mass splitting, and the mass splitting tends to increase with a decrease of  $s_4$ . Also  $m_X$  is favored to have a large value for a small  $s_4$ . Besides, the PT, whose third step is first order, tends to be achieved in the region of relatively large  $|\lambda_5|$ .

In BP1 and BP2, the 70-80 GeV lightest CP-odd scalar boson  $A$  is predicted. Because of  $\kappa_u = \kappa_\ell = 0$ ,  $\kappa_d = 0.954$  (0.891) for BP1 and BP2, the  $A$  coupling to the top quark is absent according to Eq. (14), leading to a negligible production cross section via gluon-gluon fusion



process at the LHC. The  $A$  can be mainly produced via the  $pp \rightarrow Ab\bar{b}$  process at the LHC, and then  $A$  decays into  $b\bar{b}$ . However, it is challenging to isolate potential signals from the overwhelming QCD background, and several strategies need be improved, such as precise event selection with optimized kinematic cuts, and advanced jet substructure techniques to distinguish signal-like jets from QCD jets. Additionally, the machine learning-based analyses can enhance signal-to-background discrimination.

## VI. BARYOGENESIS

We take the WKB approximation method to calculate the CP-violating source terms and chemical potentials transport equations of particle species in the wall frame with a radial coordinate  $z$  [23, 123, 124]. When a top quark penetrates the bubble wall, it acquires a complex mass as a function of  $z$ ,

$$m_t(z) = \frac{y_t}{\sqrt{2}} \sqrt{(c_\beta \varphi_1(z) + s_\beta \varphi_2(z))^2 + s_\beta^2 \varphi_3^2(z)} e^{i\Theta_t(z)} \quad (29)$$

with

$$\begin{aligned} \Theta_t(z) &= \Theta_Z(z) + \arctan \frac{s_\beta \varphi_3(z)}{c_\beta \varphi_1(z) + s_\beta \varphi_2(z)}, \partial_z \Theta_Z(z) = -\frac{\varphi_2^2(z) + \varphi_3^2(z)}{\varphi_1^2(z) + \varphi_2^2(z) + \varphi_3^2(z)} \partial_z \Theta(z), \\ \Theta(z) &= \arctan \frac{\varphi_3(z)}{\varphi_2(z)}. \end{aligned} \quad (30)$$

Because the imaginary part of the neutral element of  $\Phi_1$  is chosen to be zero in our discussions, the nonvanishing  $Z_\mu$  field produce an additional CP-violating force acting on the top quark, which is removed by a local axial transformation of top quark, reintroducing an additional overall phase  $\Theta_Z(z)$  into  $m_t$  [28].

The complex mass of the top quark drives the transport equations, which include effects of the strong sphaleron process ( $\Gamma_{ss}$ ) [23, 125], W-scattering ( $\Gamma_W$ ) [23, 126], the top Yukawa interaction ( $\Gamma_y$ ) [23, 126], the top helicity flips ( $\Gamma_M$ ) [23, 126], and the Higgs number violation

( $\Gamma_h$ ) [23, 126]. The transport equations are given by

$$\begin{aligned}
0 &= 3v_W K_{1,t} (\partial_z \mu_{t,2}) + 3v_W K_{2,t} (\partial_z m_t^2) \mu_{t,2} + 3 (\partial_z u_{t,2}) \\
&\quad - 3\Gamma_y (\mu_{t,2} + \mu_{t^c,2} + \mu_{h,2}) - 6\Gamma_M (\mu_{t,2} + \mu_{t^c,2}) - 3\Gamma_W (\mu_{t,2} - \mu_{b,2}) \\
&\quad - 3\Gamma_{ss} [(1 + 9K_{1,t}) \mu_{t,2} + (1 + 9K_{1,b}) \mu_{b,2} + (1 - 9K_{1,t}) \mu_{t^c,2}] , \\
0 &= 3v_W K_{1,t} (\partial_z \mu_{t^c,2}) + 3v_W K_{2,t} (\partial_z m_t^2) \mu_{t^c,2} + 3 (\partial_z u_{t^c,2}) \\
&\quad - 3\Gamma_y (\mu_{t,2} + \mu_{b,2} + 2\mu_{t^c,2} + 2\mu_{h,2}) - 6\Gamma_M (\mu_{t,2} + \mu_{t^c,2}) \\
&\quad - 3\Gamma_{ss} [(1 + 9K_{1,t}) \mu_{t,2} + (1 + 9K_{1,b}) \mu_{b,2} + (1 - 9K_{1,t}) \mu_{t^c,2}] , \\
0 &= 3v_W K_{1,b} (\partial_z \mu_{b,2}) + 3 (\partial_z u_{b,2}) - 3\Gamma_y (\mu_{b,2} + \mu_{t^c,2} + \mu_{h,2}) - 3\Gamma_W (\mu_{b,2} - \mu_{t,2}) , \\
&\quad - 3\Gamma_{ss} [(1 + 9K_{1,t}) \mu_{t,2} + (1 + 9K_{1,b}) \mu_{b,2} + (1 - 9K_{1,t}) \mu_{t^c,2}] , \\
0 &= 4v_W K_{1,h} (\partial_z \mu_{h,2}) + 4 (\partial_z u_{h,2}) - 3\Gamma_y (\mu_{t,2} + \mu_{b,2} + 2\mu_{t^c,2} + 2\mu_{h,2}) - 4\Gamma_h \mu_{h,2} , \\
S_t &= -3K_{4,t} (\partial_z \mu_{t,2}) + 3v_W \tilde{K}_{5,t} (\partial_z u_{t,2}) + 3v_W \tilde{K}_{6,t} (\partial_z m_t^2) u_{t,2} + 3\Gamma_t^{\text{tot}} u_{t,2} , \\
0 &= -3K_{4,b} (\partial_z \mu_{b,2}) + 3v_W \tilde{K}_{5,b} (\partial_z u_{b,2}) + 3\Gamma_b^{\text{tot}} u_{b,2} , \\
S_t &= -3K_{4,t} (\partial_z \mu_{t^c,2}) + 3v_W \tilde{K}_{5,t} (\partial_z u_{t^c,2}) + 3v_W \tilde{K}_{6,t} (\partial_z m_t^2) u_{t^c,2} + 3\Gamma_t^{\text{tot}} u_{t^c,2} , \\
0 &= -4K_{4,h} (\partial_z \mu_{h,2}) + 4v_W \tilde{K}_{5,h} (\partial_z u_{h,2}) + 4\Gamma_h^{\text{tot}} u_{h,2} . \tag{31}
\end{aligned}$$

The  $\mu_{i,2}$  and  $u_{i,2}$  are the second-order CP-odd chemical potential and the plasma velocity of the particle  $i = t, t^c, b, h$ .  $S_t$  is the source term,

$$S_t = -v_W K_{8,t} \partial_z (m_t^2 \partial_z \Theta_t) + v_W K_{9,t} (\partial_z \Theta_t) m_t^2 (\partial_z m_t^2) . \tag{32}$$

The  $\Gamma_i^{\text{tot}}$  are the total reaction rate of the particle  $i$  [23, 124], and the functions  $K_{a,i}$  and  $\tilde{K}_{a,i}$  ( $a = 1 - 9$ ) are given in Ref. [124].

We solve the transport equations with the boundary conditions  $\mu_i (z = \pm\infty) = 0$  ( $i = t, t^c, b, h$ ), and obtain the chemical potentials  $\mu_i$  and velocity perturbations  $u_i$  of each particle species. The weak sphaleron process converts the left-handed quark number into a baryon asymmetry, which is calculated as

$$Y_B = \frac{405\Gamma_{ws}}{4\pi^2 v_w g_* T_n} \int_0^\infty dz \mu_{B_L}(z) f_{sph}(z) \exp\left(-\frac{45\Gamma_{ws} z}{4v_w}\right) . \tag{33}$$

$\Gamma_{ws} \simeq 10^{-6} T_n$  is the weak sphaleron rate inside bubble [127] and  $v_w$  is the wall velocity.  $\mu_{B_L}$  is the chemical potential of left-handed quarks, and the function  $f_{sph}(z) = \min(1, 2.4 \frac{T_n}{\Gamma_{ws}} e^{-40v_n(z)/T_n})$  with  $v_n(z) = \sqrt{\langle\varphi_1(z)\rangle^2 + \langle\varphi_2(z)\rangle^2 + \langle\varphi_3(z)\rangle^2}$  is employed to smoothly interpolate between the sphaleron rate in the unbroken and broken phases [28].

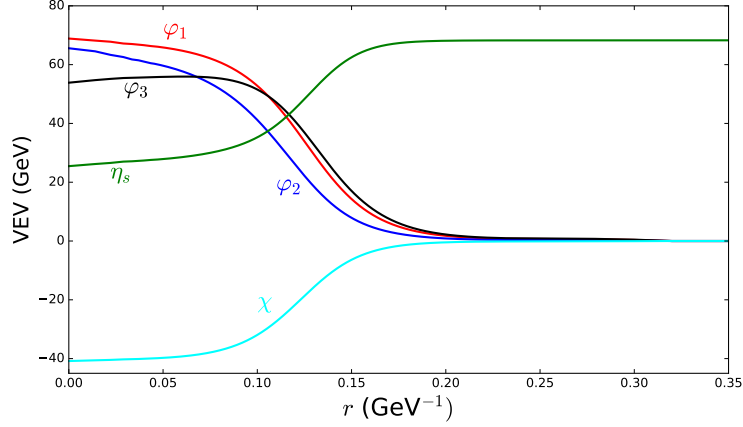


FIG. 7: The radial nucleation bubble wall VEV profiles for the second-step PT of the BP1.

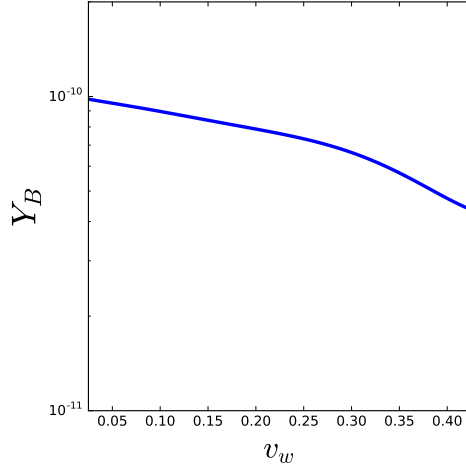


FIG. 8:  $Y_B$  as a function of  $v_w$  for the BP1.

The calculation of BAU for the BP1 depends on the bubble wall profiles for the second-step PT, and they are given in Fig. 7. The WKB method of calculating transport equations needs the condition of  $L_W T_n \gg 1$ , where  $L_W$  is the width of bubble wall. The  $L_W T_n$  for the BP1 is approximately estimated to be 2.6. Fig. 8 displays  $Y_B$  as a function of the wall velocity  $v_w$  for the BP1.  $Y_B$  tends to decrease with an increase of  $v_w$ , and  $8 \times 10^{-11} < Y_B < 10 \times 10^{-11}$  for  $0.025 < v_w < 0.19$ .

## VII. CONCLUSION

In this work we studied a complex singlet scalar extension of the 2HDM in which the 95.4 GeV Higgs is from the mixing of three CP-even Higgs fields, and there is a mixing between the two CP-odd Higgs fields. Considering relevant theoretical and experimental

constraints, we found that the model can simultaneously explain the diphoton and  $b\bar{b}$  excesses at the 95.4 GeV while achieving spontaneous CP-violation at the finite temperature. Some strong dependencies among several key parameters are displayed. Finally, we picked out a benchmark point accommodating the diphoton and  $b\bar{b}$  excesses simultaneously, and found that the model can explain BAU while satisfying the bound of EDM.

### Acknowledgment

This work was supported by the National Natural Science Foundation of China under grant 11975013 and by the project ZR2024MA001 and ZR2023MA038 supported by Shandong Provincial Natural Science Foundation.

- 
- [1] P. A. Zyla et al. [Particle Data Group], Review of Particle Physics, PTEP **2020**, 083C01 (2020).
  - [2] A. D. Sakharov, Violation of CP Invariance, C asymmetry, and baryon asymmetry of the universe, Pisma Zh. Eksp. Teor. Fiz. **5**, 32-35 (1967).
  - [3] V. A. Kuzmin, V.A. Rubakov, M. E. Shaposhnikov, V. A. Rubakov, and M. E. Shaposhnikov, On anomalous electroweak baryon-number non-conservation in the early universe, Phys. Lett. B **155**, 36 (1985).
  - [4] V. A. Rubakov, M. E. Shaposhnikov, Usp. Fiz. Nauk **166**, 493 (1996); Phys. Usp. **39**, 461 (1996).
  - [5] J. McDonald, Electroweak baryogenesis and dark matter via a gauge singlet scalar, Phys. Lett. B **323**, 339 (1994).
  - [6] G. C. Branco, D. Delepine, D. Emmanuel-Costa and F.R. Gonzalez, Electroweak baryogenesis in the presence of an isosinglet quark, Phys. Lett. B **442**, 229 (1998).
  - [7] V. Barger, P. Langacker, M. McCaskey, M. Ramsey-Musolf and G. Shaughnessy, Complex Singlet Extension of the Standard Model, Phys. Rev. D **79**, 015018 (2009).
  - [8] S. Profumo, M. J. Ramsey-Musolf and G. Shaughnessy, Singlet Higgs phenomenology and the electroweak phase transition, JHEP **08**, 010 (2007).

- [9] M. L. Xiao and J. H. Yu, “Electroweak baryogenesis in a scalar-assisted vectorlike fermion model,” *Phys. Rev. D* **94** (2016), 015011.
- [10] F. P. Huang, Z. Qian and M. Zhang, Exploring dynamical CP violation induced baryogenesis by gravitational waves and colliders, *Phys. Rev. D* **98**, 015014 (2018).
- [11] A. Beniwal, M. Lewicki, M. White and A. G. Williams, “Gravitational waves and electroweak baryogenesis in a global study of the extended scalar singlet model,” *JHEP* **02** (2019), 183.
- [12] M. Jiang, L. Bian, W. Huang and J. Shu, Impact of a complex singlet: Electroweak baryogenesis and dark matter, *Phys. Rev. D* **93**, 065032 (2016).
- [13] P. H. Ghorbani, Electroweak Baryogenesis and Dark Matter via a Pseudoscalar vs. Scalar, *JHEP* **08**, 058 (2017).
- [14] W. Chao, CP Violation at the Finite Temperature, *Phys. Lett. B* **796** (2019), 102-106.
- [15] B. Grzadkowski and D. Huang, Spontaneous  $CP$ -Violating Electroweak Baryogenesis and Dark Matter from a Complex Singlet Scalar, *JHEP* **08**, 135 (2018).
- [16] K. P. Xie, Lepton-mediated electroweak baryogenesis, gravitational waves and the  $4\tau$  final state at the collider, *JHEP* **02**, 090 (2021) [erratum: *JHEP* **8**, 052 (2022)].
- [17] M. Lewicki, M. Merchand and M. Zych, Electroweak bubble wall expansion: gravitational waves and baryogenesis in Standard Model-like thermal plasma, *JHEP* **02**, 017 (2022).
- [18] J. Ellis, M. Lewicki, M. Merchand, J. M. No and M. Zych, The scalar singlet extension of the Standard Model: gravitational waves versus baryogenesis, *JHEP* **01**, 093 (2023).
- [19] C. Idegawa and E. Senaha, “Electron electric dipole moment and electroweak baryogenesis in a complex singlet extension of the Standard Model with degenerate scalars,” [arXiv:2309.09430 [hep-ph]].
- [20] K. Harigaya and I. R. Wang, “First-Order Electroweak Phase Transition and Baryogenesis from a Naturally Light Singlet Scalar,” [arXiv:2207.02867 [hep-ph]].
- [21] N. Turok and J. Zadrozny, Electroweak baryogenesis in the two doublet model, *Nucl. Phys. B* **358**, 471-493 (1991).
- [22] J. M. Cline, K. Kainulainen and A. P. Vischer, Dynamics of two Higgs doublet CP violation and baryogenesis at the electroweak phase transition, *Phys. Rev. D* **54**, 2451-2472 (1996).
- [23] L. Fromme, S. J. Huber and M. Seniuch, Baryogenesis in the two-Higgs doublet model, *JHEP* **11**, 038 (2006).
- [24] S. Kanemura, Y. Okada and E. Senaha, “Electroweak baryogenesis and quantum corrections

- to the triple Higgs boson coupling,” *Phys. Lett. B* **606** (2005), 361-366.
- [25] P. Basler, M. Mühlleitner and J. Wittbrodt, “The CP-Violating 2HDM in Light of a Strong First Order Electroweak Phase Transition and Implications for Higgs Pair Production,” *JHEP* **03** (2018), 061.
  - [26] T. Abe, J. Hisano, T. Kitahara and K. Tobioka, “Gauge invariant Barr-Zee type contributions to fermionic EDMs in the two-Higgs doublet models,” *JHEP* **01** (2014), 106; [erratum: *JHEP* **04** (2016), 161].
  - [27] S. Tulin and P. Winslow, Anomalous B meson mixing and baryogenesis, *Phys. Rev. D* **84**, 034013 (2011).
  - [28] J. M. Cline, K. Kainulainen and M. Trott, Electroweak Baryogenesis in Two Higgs Doublet Models and B meson anomalies, *JHEP* **11**, 089 (2011).
  - [29] T. Liu, M. J. Ramsey-Musolf and J. Shu, Electroweak Beautygenesis: From  $b \rightarrow s$  CP-violation to the Cosmic Baryon Asymmetry, *Phys. Rev. Lett.* **108**, 221301 (2012).
  - [30] M. Ahmadvand, Baryogenesis within the two-Higgs-doublet model in the Electroweak scale, *Int. J. Mod. Phys. A* **29**, 1450090 (2014).
  - [31] C. W. Chiang, K. Fuyuto and E. Senaha, Electroweak Baryogenesis with Lepton Flavor Violation, *Phys. Lett. B* **762**, 315 (2016).
  - [32] H. K. Guo, Y. Y. Li, T. Liu, M. Ramsey-Musolf and J. Shu, Lepton-Flavored Electroweak Baryogenesis, *Phys. Rev. D* **96**, 115034 (2017).
  - [33] T. Modak and E. Senaha, Electroweak baryogenesis via bottom transport, *Phys. Rev. D* **99**, 115022 (2019).
  - [34] P. Basler, M. Mühlleitner and J. Müller, BSMPT v2 a tool for the electroweak phase transition and the baryon asymmetry of the universe in extended Higgs Sectors, *Comput. Phys. Commun.* **269**, 108124 (2021).
  - [35] S. F. Ge, G. Li, P. Pasquini and M. J. Ramsey-Musolf, “CP-violating Higgs Di-tau Decays: Baryogenesis and Higgs Factories,” *Phys. Rev. D* **103** (2021), 095027.
  - [36] R. Zhou, L. Bian, Gravitational wave and electroweak baryogenesis with two Higgs doublet models, *Phys. Lett. B* **829**, 137105 (2022).
  - [37] P. Basler, M. Mühlleitner and J. Müller, Electroweak Baryogenesis in the CP-Violating Two-Higgs Doublet Model, *Eur. Phys. J. C* **83**, 57 (2023).
  - [38] K. Enomoto, S. Kanemura, Y. Mura, Electroweak baryogenesis in aligned two Higgs doublet

- models, JHEP **01**, 104 (2022).
- [39] K. Enomoto, S. Kanemura, Y. Mura, New benchmark scenarios of electroweak baryogenesis in aligned two Higgs double models, JHEP **09**, 121 (2022).
  - [40] D. Gonçalves, A. Kaladharan and Y. Wu, “Gravitational waves, bubble profile, and baryon asymmetry in the complex 2HDM, Phys. Rev. D **108** (2023), 075010.
  - [41] Y. Z. Li, M. J. Ramsey-Musolf and J. H. Yu, “Does the Electron EDM Preclude Electroweak Baryogenesis ?,” arXiv:2404.19197.
  - [42] ACME collaboration, J. Baron et al., Order of Magnitude Smaller Limit on the Electric Dipole Moment of the Electron, Science **343**, 269 (2014).
  - [43] S. J. Huber, K. Mimasu and J. M. No, Baryogenesis from spontaneous CP violation in the early Universe, Phys. Rev. D **107**, (2023) 075042.
  - [44] S. Liu and L. Wang, “Spontaneous CP violation electroweak baryogenesis and gravitational wave through multistep phase transitions,” Phys. Rev. D **107** (2023), 115008.
  - [45] J. Ma, J. Wang and L. Wang, “Electroweak baryogenesis, dark matter, and dark CP symmetry,” Phys. Rev. D **109** (2024), 075024.
  - [46] CMS collaboration, “Search for a standard model-like Higgs boson in the mass range between 70 and 110 GeV in the diphoton final state in proton-proton collisions at  $\sqrt{s} = 13$  TeV,” CMS-PAS-HIG-20-002, 2023.
  - [47] C. Arcangeletti. on behalf of ATLAS collaboration, LHC Seminar <https://indico.cern.ch/event/1281604/attachments/2660420/4608571/LHCSeminarArcangeletti.final.pdf>, 7<sup>th</sup> of June, 2023.
  - [48] T. Biekötter, S. Heinemeyer and G. Weiglein, “95.4 GeV diphoton excess at ATLAS and CMS,” Phys. Rev. D **109** (2024), 3.
  - [49] R. Barate *et al.* [LEP Working Group for Higgs boson searches, ALEPH, DELPHI, L3 and OPAL], “Search for the standard model Higgs boson at LEP,” Phys. Lett. B **565** (2003), 61-75.
  - [50] J. Cao, X. Guo, Y. He, P. Wu and Y. Zhang, “Diphoton signal of the light Higgs boson in natural NMSSM,” Phys. Rev. D **95** (2017), 116001.
  - [51] T. Biekötter, M. Chakraborti and S. Heinemeyer, “A 96 GeV Higgs boson in the N2HDM,” Eur. Phys. J. C **80** (2020), 2.
  - [52] S. Heinemeyer, C. Li, F. Lika, G. Moortgat-Pick and S. Paasch, “Phenomenology of a 96 GeV

- Higgs boson in the 2HDM with an additional singlet,” *Phys. Rev. D* **106** (2022), 075003.
- [53] T. Biekötter, S. Heinemeyer and G. Weiglein, “Mounting evidence for a 95 GeV Higgs boson,” *JHEP* **08** (2022), 201.
  - [54] J. A. Aguilar-Saavedra, H. B. Câmara, F. R. Joaquim and J. F. Seabra, “Confronting the 95 GeV excesses within the  $U(1)$ ’-extended next-to-minimal 2HDM,” *Phys. Rev. D* **108** (2023), 075020.
  - [55] K. Choi, S. H. Im, K. S. Jeong and C. B. Park, “Light Higgs bosons in the general NMSSM,” *Eur. Phys. J. C* **79** (2019), 956.
  - [56] S. Ma, K. Wang and J. Zhu, “Higgs decay to light (pseudo)scalars in the semi-constrained NMSSM,” *Chin. Phys. C* **45** (2021), 023113.
  - [57] W. Li, H. Qiao and J. Zhu, “Light Higgs boson in the NMSSM confronted with the CMS di-photon and di-tau excesses,” *Chin. Phys. C* **47** (2023), 123102.
  - [58] U. Ellwanger and C. Hugonie, “Additional Higgs Bosons near 95 and 650 GeV in the NMSSM,” *Eur. Phys. J. C* **83** (2023), 1138.
  - [59] P. S. B. Dev, R. N. Mohapatra and Y. Zhang, “Explanation of the 95 GeV  $\gamma\gamma$  and  $b\bar{b}$  excesses in the minimal left-right symmetric model,” *Phys. Lett. B* **849** (2024), 138481.
  - [60] C. Bonilla, A. E. Carcamo Hernandez, S. Kovalenko, H. Lee, R. Pasechnik and I. Schmidt, “Fermion mass hierarchy in an extended left-right symmetric model,” *JHEP* **12** (2023), 075.
  - [61] C. X. Liu, Y. Zhou, X. Y. Zheng, J. Ma, T. F. Feng and H. B. Zhang, “95 GeV excess in a CP-violating  $\mu$ -from- $\nu$  SSM,” *Phys. Rev. D* **109** (2024), 056001.
  - [62] W. Li, H. Qiao, K. Wang and J. Zhu, “Light dark matter confronted with the 95 GeV diphoton excess,” arXiv:2312.17599.
  - [63] G. Abbas and N. Singh, “Dark-technicolour at low scale,” arXiv:2312.16532.
  - [64] A. Ahriche, M. L. Bellilet, M. O. Khojali, M. Kumar and A. T. Mulaudzi, “The scale invariant scotogenic model: CDF-II  $W$ -boson mass and the 95 GeV excesses,” arXiv:2311.08297.
  - [65] J. Cao, X. Jia, J. Lian and L. Meng, “95 GeV diphoton and  $b\bar{b}$  excesses in the general next-to-minimal supersymmetric standard model,” *Phys. Rev. D* **109** (2024), 075001.
  - [66] M. Maniatis and O. Nachtmann, “CMS results for the  $\gamma\gamma$  production at the LHC: do they give a hint for a Higgs boson of the maximally CP symmetric two-Higgs-doublet model?,” arXiv:2309.04869.
  - [67] A. Belyaev, R. Benbrik, M. Boukidi, M. Chakraborti, S. Moretti and S. Semmlali, “Explanation



- of the hints for a 95 GeV Higgs boson within a 2-Higgs Doublet Model,” *JHEP* **05** (2024), 209.
- [68] D. Azevedo, T. Biekötter and P. M. Ferreira, “2HDM interpretations of the CMS diphoton excess at 95 GeV,” *JHEP* **11** (2023), 017.
  - [69] D. Bhatia, N. Desai and S. Dwivedi, “Discovery prospects of a light charged Higgs near the fermiophobic region of Type-I 2HDM,” *JHEP* **06** (2023), 100.
  - [70] T. K. Chen, C. W. Chiang, S. Heinemeyer and G. Weiglein, “95 GeV Higgs boson in the Georgi-Machacek model,” *Phys. Rev. D* **109** (2024), 075043.
  - [71] A. Ahriche, “The 95 GeV Excess in the Georgi-Machacek Model: Single or Twin Peak Resonance,” arXiv:2312.10484.
  - [72] G. Arcadi, G. Busoni, D. Cabo-Almeida and N. Krishnan, “Is there a (Pseudo)Scalar at 95 GeV?,” arXiv:2311.14486.
  - [73] D. Borah, S. Mahapatra, P. K. Paul and N. Sahu, “Scotogenic  $U(1)_{L\mu-L\tau}$  origin of  $(g-2)\mu$ , W-mass anomaly and 95 GeV excess,” *Phys. Rev. D* **109** (2024), 055021.
  - [74] S. Banik, G. Coloretti, A. Crivellin and B. Mellado, “Uncovering New Higgses in the LHC Analyses of Differential  $t\bar{t}$  Cross Sections,” arXiv:2308.07953.
  - [75] J. Dutta, J. Lahiri, C. Li, G. Moortgat-Pick, S. F. Tabira and J. A. Ziegler, “Dark Matter Phenomenology in 2HDMS in light of the 95 GeV excess,” arXiv:2308.05653.
  - [76] S. Bhattacharya, G. Coloretti, A. Crivellin, S. E. Dahbi, Y. Fang, M. Kumar and B. Mellado, “Growing Excesses of New Scalars at the Electroweak Scale,” arXiv:2306.17209.
  - [77] S. Ashanujjaman, S. Banik, G. Coloretti, A. Crivellin, B. Mellado and A. T. Mulaudzi, “ $SU(2)_L$  triplet scalar as the origin of the 95 GeV excess?,” *Phys. Rev. D* **108** (2023), L091704.
  - [78] P. Escribano, V. M. Lozano and A. Vicente, “Scotogenic explanation for the 95 GeV excesses,” *Phys. Rev. D* **108** (2023), 115001.
  - [79] T. Biekötter, S. Heinemeyer and G. Weiglein, “The CMS di-photon excess at 95 GeV in view of the LHC Run 2 results,” *Phys. Lett. B* **846** (2023), 138217.
  - [80] S. Banik, A. Crivellin, S. Iguro and T. Kitahara, “Asymmetric di-Higgs signals of the next-to-minimal 2HDM with a  $U(1)$  symmetry,” *Phys. Rev. D* **108** (2023), 075011.
  - [81] G. Coloretti, A. Crivellin, S. Bhattacharya and B. Mellado, “Searching for low-mass resonances decaying into W bosons,” *Phys. Rev. D* **108** (2023), 035026.

- [82] A. Ahriche, “Constraining the Georgi-Machacek model with a light Higgs boson,” *Phys. Rev. D* **107** (2023), 015006.
- [83] R. Benbrik, M. Boukidi, S. Moretti and S. Semmlali, “Explaining the 96 GeV Di-photon anomaly in a generic 2HDM Type-III,” *Phys. Lett. B* **832** (2022), 137245.
- [84] T. Biekötter, S. Heinemeyer and G. Weiglein, “Excesses in the low-mass Higgs-boson search and the  $W$ -boson mass measurement,” *Eur. Phys. J. C* **83** (2023), 450.
- [85] T. Biekötter, A. Grohsjean, S. Heinemeyer, C. Schwanenberger and G. Weiglein, “Possible indications for new Higgs bosons in the reach of the LHC: N2HDM and NMSSM interpretations,” *Eur. Phys. J. C* **82** (2022), 178.
- [86] A. A. Abdelalim, B. Das, S. Khalil and S. Moretti, “Di-photon decay of a light Higgs state in the BLSSM,” *Nucl. Phys. B* **985** (2022), 116013.
- [87] T. Biekötter, M. Chakraborti and S. Heinemeyer, “The “96 GeV excess” at the LHC,” *Int. J. Mod. Phys. A* **36** (2021), 2142018.
- [88] J. A. Aguilar-Saavedra and F. R. Joaquim, “Multiphoton signals of a (96 GeV?) stealth boson,” *Eur. Phys. J. C* **80** (2020), 403.
- [89] J. Cao, X. Jia, Y. Yue, H. Zhou and P. Zhu, “96 GeV diphoton excess in seesaw extensions of the natural NMSSM,” *Phys. Rev. D* **101** (2020), 055008.
- [90] A. Kundu, S. Maharana and P. Mondal, “A 96 GeV scalar tagged to dark matter models,” *Nucl. Phys. B* **955** (2020), 115057.
- [91] J. Cao, X. Jia and J. Lian, “Unified Interpretation of Muon  $g-2$  anomaly, 95 GeV Diphoton, and  $b\bar{b}$  Excesses in the General Next-to-Minimal Supersymmetric Standard Model,” *arXiv:2402.15847*.
- [92] J. Kalinowski and W. Kotlarski, “Interpreting 95 GeV di-photon/ $b\bar{b}$  excesses as a lightest Higgs boson of the MRSSM,” *JHEP* **07** (2024), 037.
- [93] U. Ellwanger, C. Hugonie, S. F. King and S. Moretti, “NMSSM Explanation for Excesses in the Search for Neutralinos and Charginos and a 95 GeV Higgs Boson,” *arXiv:2404.19338*.
- [94] R. Benbrik, M. Boukidi and S. Moretti, “Superposition of CP-Even and CP-Odd Higgs Resonances: Explaining the 95 GeV Excesses within a Two-Higgs Doublet Model,” *arXiv:2405.02899*.
- [95] J. Lian, “The 95GeV Excesses in the  $\mathbb{Z}_3$ -symmetric Next-to Minimal Supersymmetric Standard Model,” *arXiv:2406.10969*.

- [96] J. L. Yang, M. H. Guo, W. H. Zhang, H. B. Zhang and T. F. Feng, “Explaining the possible 95 GeV excesses in the  $B - L$  symmetric SSM,” arXiv:2406.01926.
- [97] A. Pich, P. Tuzon, Yukawa Alignment in the Two-Higgs-Doublet Model, Phys. Rev. D **80**, (2009) 091702.
- [98] L. Wang and X. F. Han, Status of the aligned two-Higgs-doublet model confronted with the Higgs data, JHEP **04**, 128 (2014).
- [99] H. Bahl, T. Biekötter, S. Heinemeyer, C. Li, S. Paasch, G. Weiglein and J. Wittbrodt, “HiggsTools: BSM scalar phenomenology with new versions of HiggsBounds and HiggsSignals,” Comput. Phys. Commun. **291** (2023), 108803.
- [100] P. Bechtle, S. Heinemeyer, O. Stål, T. Stefaniak and G. Weiglein, “*HiggsSignals*: Confronting arbitrary Higgs sectors with measurements at the Tevatron and the LHC,” Eur. Phys. J. C **74** (2014), 2711.
- [101] P. Bechtle, D. Dercks, S. Heinemeyer, T. Klingl, T. Stefaniak, G. Weiglein and J. Wittbrodt, “HiggsBounds-5: Testing Higgs Sectors in the LHC 13 TeV Era,” Eur. Phys. J. C **80** (2020), 1211.
- [102] P. Bechtle, O. Brein, S. Heinemeyer, G. Weiglein and K. E. Williams, “HiggsBounds: Confronting Arbitrary Higgs Sectors with Exclusion Bounds from LEP and the Tevatron,” Comput. Phys. Commun. **181** (2010), 138-167.
- [103] F. Mahmoudi, “SuperIso v2.3: A Program for calculating flavor physics observables in Supersymmetry,” Comput. Phys. Commun. **180** (2009), 1579-1613.
- [104] K. Kannike, “Vacuum Stability Conditions From Copositivity Criteria,” Eur. Phys. J. C **72** (2012), 2093.
- [105] W. Porod, “SPHeno, a program for calculating supersymmetric spectra, SUSY particle decays and SUSY particle production at  $e^+ e^-$  colliders, Comput. Phys. Commun. **153** (2003), 275-315.
- [106] F. Staub, “SARAH 4 : A tool for (not only SUSY) model builders,” Comput. Phys. Commun. **185** (2014), 1773-1790.
- [107] H.-J. He, N. Polonsky, S. Su, Extra families, Higgs spectrum and oblique corrections, Phys. Rev. D **64**, (2001) 053004.
- [108] H. E. Haber, D. O’Neil, Basis-independent methods for the two-Higgs-doublet model. III. The CP-conserving limit, custodial symmetry, and the oblique parameters S, T, U, Phys. Rev. D

**83**, (2011) 055017.

- [109] R. Jackiw, Functional evaluation of the effective potential, *Phys. Rev. D* **9**, 1686 (1974).
- [110] H. H. Patel and M. J. Ramsey-Musolf, Baryon Washout, Electroweak Phase Transition, and Perturbation Theory, *JHEP* **07**, 029 (2011).
- [111] S. R. Coleman and E. J. Weinberg, Radiative Corrections as the Origin of Spontaneous Symmetry Breaking, *Phys. Rev. D* **7**, 1888 (1973).
- [112] L. Dolan and R. Jackiw, Symmetry Behavior at Finite Temperature, *Phys. Rev. D* **9**, 3320 (1974).
- [113] P. B. Arnold and O. Espinosa, The Effective potential and first order phase transitions: Beyond leading-order, *Phys. Rev. D* **47**, 3546 (1993) [Erratum: *Phys. Rev. D* **50**, 6662 (1994)].
- [114] R. R. Parwani, Resummation in a hot scalar field theory, *Phys. Rev. D* **45**, 4695 (1992).
- [115] I. Affleck, Quantum Statistical Metastability, *Phys. Rev. Lett.* **46**, 388 (1981).
- [116] A. D. Linde, Decay of the False Vacuum at Finite Temperature, *Nucl. Phys. B* **216**, 421 (1983) [Erratum: *Nucl. Phys. B* **223**, 544 (1983)].
- [117] A. D. Linde, Fate of the False Vacuum at Finite Temperature: Theory and Applications, *Phys. Lett. B* **100**, 37-40 (1981).
- [118] A. D. Linde, Fate of the False Vacuum at Finite Temperature: Theory and Applications, *Phys. Lett. B* **100**, 37-40 (1981).
- [119] V. Guada, M. Nemevšek and M. Pintar, FindBounce: Package for multi-field bounce actions, *Comput. Phys. Commun.* **256**, 107480 (2020).
- [120] J. R. Espinosa, B. Gripaios, T. Konstandin, and F. Riva, Electroweak Baryogenesis in Non-minimal Composite Higgs Models, *JCAP* **01**, 012 (2012).
- [121] C. L. Wainwright, CosmoTransitions: Computing Cosmological Phase Transition Temperatures and Bubble Profiles with Multiple Fields, *Computl. Phys. Commun.* **183**, 2006-2013 (2012).
- [122] G. D. Moore, Measuring the broken phase sphaleron rate nonperturbatively, *Phys. Rev. D* **59**, 014503 (1999).
- [123] J. M. Cline, M. Joyce and K. Kainulainen, Supersymmetric electroweak baryogenesis, *JHEP* **07**, 018 (2000).
- [124] L. Fromme and S. J. Huber, Top transport in electroweak baryogenesis, *JHEP* **03**, 049

- (2007).
- [125] G. F. Giudice and M. E. Shaposhnikov, Strong sphalerons and electroweak baryogenesis, Phys. Lett. B **326**, 118-124 (1994).
- [126] P. Huet and A. E. Nelson, "Electroweak baryogenesis in supersymmetric models," Phys. Rev. D **53**, 4578 (1996).
- [127] G. D. Moore, Sphaleron rate in the symmetric electroweak phase, Phys. Rev. D **62**, 085011 (2000).